Lawrence Berkeley National Laboratory
LBL Publications

Title

Self-Potential Anomaly Changes at the Cerro Prieto Geothermal Field

Permalink

https://escholarship.org/uc/item/4rd0h4r3

Authors

Goldstein, N E

Alvarez R, J

Publication Date

1989-04-01

Lawrence Berkeley Laboratory

UNIVERSITY OF CALIFORNIA

EARTH SCIENCES DIVISION

Self-Potential Anomaly Changes at the Cerro Prieto Geothermal Field

N.E. Goldstein and J. Alvarez R.

April 1989

DISCLAIMER

Self-Potential Anomaly Changes at the Cerro Prieto Geothermal Field

N.E. Goldstein* and J. Alvarez R.‡

*Earth Sciences Division
Lawrence Berkeley Laboratory
1 Cyclotron Road
Berkeley, California 94720

‡Coordinadora Ejecutiva de Cerro Prieto
Comisión Federal de Electricidad de Mexico
Mexicali, B.C., Mexico

April 1989

Self-Potential Anomaly Changes at the
Cerro Prieto Geothermal Field

N. E. Goldstein* and J. Alvarez R.‡

*Earth Sciences Division, Lawrence Berkeley Laboratory,
University of California, Berkeley, California 94720

‡ Coordinadora Ejecutiva de Cerro Prieto,
Comisión Federal de Electricidad, Mexicali, B.C., Mexico

Abstract

CFE conducted a repeat self-potential (SP) survey over the Cerro Prieto geothermal field during March 1988, ten years after the original survey. This gave us an unprecedented opportunity to see whether SP changes have occurred and to test whether the changes are related to production.

The axis of the approximately dipolar anomaly has shifted 2 km eastward, and we were able to match one profile line across the observed SP anomaly to a 2-D electrokinetic model based on actual production rates and a hydrogeology model established from drill hole logs and well completion data. A series of calculations show the sensitivity of the calculated SP to recharge source magnitudes and locations.

Notwithstanding the sources of uncertainty in the numerical model, it appears that the SP effect can be explained by β reservoir production with lateral recharge from the east and southeast. Some of the recharge occurs in the unconsolidated sediments of the upper 1 km, which fits with the model of recharge to the shallow α reservoir in the CPI area. There also seems to be a component of natural deep recharge in the Z sand unit that is approximately equal to production from the downthrown side of the β reservoir. However, the SP data can be fitted to an electrokinetic model without a pressure source simulating recharge to the upthrown side of the β reservoir. This finding is in agreement with independent reservoir studies and well production data which show a deficiency of fluid recharge in the northeastern CPIII production area.

Other SP calculations indicate that surface potentials due to the heat source are of the order of only 3 mV, or within the noise level of the data. As suggested by resistivity measurements and the hydrogeology, a liquid junction diffusion potential may be present due to ionic diffusion between high salinity thermal fluids in contact with less saline groundwaters. Calculations indicate that the peak-to-peak voltage variation from this phenomenon can be of the order of 10 to 15 mV if the contact zone comes close to the surface. If this phenomenon is actually occurring in the field, its SP anomaly when added to the electrokinetic SP anomaly should provide a slightly better match to the observed SP data.

Resumen

En marzo de 1988, 10 años después del primer levantamiento de potencial natural en el campo geotérmico de Cerro Prieto, CFE realizó un nuevo estudio de este tipo. Esto nos dió la rara oportunidad de establecer si ocurrieron cambios en el potencial natural y de evaluar si dichos cambios están relacionados con la explotación del campo.

El eje de la anomalía aproximadamente dipolar se ha desplazado 2 km hacia el este. Se obtuvo una correspondencia entre un perfil que cruza la anomalía observada de potencial natural y un modelo bidimensional electrocinético basado en datos reales de producción y en un modelo hidrogeológico desarrollado usando registros y datos de terminación de pozos. Una serie de cómputos muestra la sensitividad del potencial natural calculado a la magnitud y localización de las fuentes de recarga.

A pesar de las incertidumbres asociadas con el modelo numérico, parecería que el efecto de potencial natural podría ser explicado por la explotación del yacimiento β y la recarga lateral proveniente del este y sudeste. Parte de la recarga ocurre en los sedimentos no consolidados que se encuentran a menos de un kilómetro de profundidad, lo que concuerda con el modelo de recarga del yacimiento somero α de CPI. También parece existir una componente de recarga natural profunda en la unidad arenosa Z, la que es aproximadamente igual a la producción asociada con el bloque hundido del yacimiento β. Sin embargo los datos de potencial natural pueden ser ajustados a un modelo electrocinético que no presenta una fuente de presión simulando la recarga del bloque levantado del yacimiento β. Estos resultados están de acuerdo con estudios independientes de yacimento y con datos de producción de pozos, los que indican una insuficiencia en la recarga de fluidos al área de CPIII.

Otros calculos de potencial natural indican que los voltajes medidos en superficie debidos a una fuente de calor son sólo del orden de 3 mV, o sea dentro del intervalo de ruido de los datos. Las mediciones de resistividad y el modelo hidrogeológico sugieren la generación de un potencial natural debido a difusión iónica entre aguas geotérmicas de alta salinidad y aguas subterráneas de menor salinidad. Si la zona de contacto entre estas aguas se encuentra cerca de la superficie, las variaciones de tensión cresta a cresta asociadas con este fenómeno podrían ser del orden de 10 a 15 mV. Si suponemos la existencia de este proceso en el campo y sumamos esta anomalía de potencial natural a la anomalía electrocinética, se mejora un poco la concordancia entre los potenciales naturales observados y calculados.

Introduction

Most geothermal fields are reported to have an associated self-potential (SP) anomaly of tens to over several hundred millivolts (Corwin and Hoover, 1979). Although the interpretation of these voltages has proved difficult in the past

due to the multiplicity of causes (e.g., electrokinetic, thermoelectric, and chemical diffusion effects), lack of laboratory and field data, and the lack of interpretative techniques, recent advances indicate that the main mechanism is related to the electrokinetic effect. That is, streaming potentials are generated by subsurface flows of water, both natural and induced by geothermal fluid extraction and injection activities (Ishido et al., 1983; Ishido et al., 1987). SP monitoring near individual geothermal production and injection wells show that changes of 5 to 10 mV occur as the wells are subjected to short-term flow and injection tests (Ishido et al., 1983; Sill, 1983a). Although the voltage changes are close to the noise level of ± 5 mV encountered in a typical SP survey, the voltage anomalies over a large multi-well geothermal field would be many times larger.

An unprecedented opportunity to study production-related SP effects occurred when CFE carried out a second SP survey over the Cerro Prieto geothermal field in March 1988. A SP survey had been run ten years earlier (Corwin et al., 1978), and thus it was also hoped that the repeat survey would show changes correlative to changes in production activities.

Data Acquisition Procedures

Attempts were made to resurvey the field in the same fashion as the original survey, but this was impossible to do exactly for the reasons discussed in this section. Surveys were rerun along most of the same lines and with the same type of equipment; copper-copper sulfate electrodes and a 10-Mohm impedance digital multimeter. However, because of the expansion of surface facilities some survey lines had to be relocated, and other lines were extended for coverage over the newer production areas. Telluric noise monitoring was carried out during surveys to check for periods of anomalously strong noise.

Data acquisition techniques used at Cerro Prieto consisted of both the fixed reference and the less desirable "leapfrog" technique. The 1978 survey was conducted almost entirely using the reference electrode technique; one electrode was set at a base station and voltages were read between it and a second electrode which was moved to stations 100 to 350 m apart along a line. Due to the increased cultural activity and loss of easy access to some areas, the 1988 survey was done entirely using the leapfrog method with a 100-m measuring dipole (Arellano and Rodríguez, 1989). In the leapfrog method both electrodes move in alternating fashion along the survey line. Voltages obtained with the leapfrog method are highly susceptible to cumulative random errors, and so a great deal of effort must be made to distribute errors around polygonal loops formed by the intersections of survey lines.

The corrected voltages were smoothed by means of a 5-point moving average to help suppress small voltage perturbations due to various noise sources, such as telluric noise, man-made electrical noise, and background geologic noise due to point-to-point variations in soil moisture and chemistry. Averaging preserves the long spatial wavelengths in the data, but it changes individual readings by up to 20-30 mV. The smoothed data sets (Fig. 1 and 2) were then hand contoured. The new SP contour map displays more detail than the original map. This is due to the closer station spacing and the additional (fill-in) survey lines. Such differences make direct comparisons of the results difficult. Another consideration when comparing the two surveys is the difference in background voltage levels. This difference may be due simply to the choice of reference station.

Results

The initial SP survey was conducted in late 1977 and early 1978 when production was limited to the shallow α reservoir. At that time approximately 12 wells were producing 750 tonnes/hr (≈250 L/s) from a reservoir region 1.0 to 1.4 km below the surface. Steam separated at the wellheads was delivered to the original 75 MWe plant (Units I and II of the CPI plant). The SP contours (Fig. 1) showed a well-defined dipolar anomaly, with a peak-to-peak voltage of 160 mV, and a N-S axis centered over the original production area (Corwin et al., 1978). Qualitatively, the dipolar anomaly in Figure 1 may be explained in terms of ascending fluids recharging the production zone via the "sandy gap" of the otherwise impermeable O Shale unit (Halfman et al., 1986a). The second SP survey was carried out by Jorge Rodríguez Bahena of CFE in March 1988. At that time the installed electric generating capacity had been increased to 620 MWe with the expansion of the western CPI plant and the later addition of two new 220 MWe plants (CPII and CPIII) in the eastern parts of the field. Most of the steam for the three plants was provided by brine from deeper reservoir regions, primarily that part of the β reservoir located east of the original production area (Halfman et al., 1986a; 1986b). Brine reinjection has been insignificant during the period between SP surveys. Not unexpectedly, the 1988 survey (Fig. 2) reveals that the SP anomaly has changed in shape and position:

(1) the anomaly shape is more irregular and its dipolar form is less clear,

(2) the steepest SP gradients have shifted eastward a distance of over 2 km to a position that appears to correlate with the trace of Fault H at the depth of the β reservoir (Halfman et al., 1986b), and

(3) the peak-to-peak voltage amplitude has increased up to 20% along some lines.

Interpretation of the Cerro Prieto Data

Liquid Junction Potential

Figure 3 shows the 1988 SP contours with respect to resistivity in the 500 to 1500 m depth range, as interpreted from CFE's Schlumberger resistivity soundings. The strong east-west gradient in the resistivity contours probably reflects the difference between less saline Colorado River water to the east in contrast to the area of thermal water discharge on the west. One cannot fail to notice the excellent spatial agreement between the steepest gradients in the SP and resistivity data sets. This suggests that the SP anomaly may be due (in part) to a liquid junction diffusion potential; i.e., a potential arising from the different mobilities of cations and anions diffusing from zones of high to low concentration.
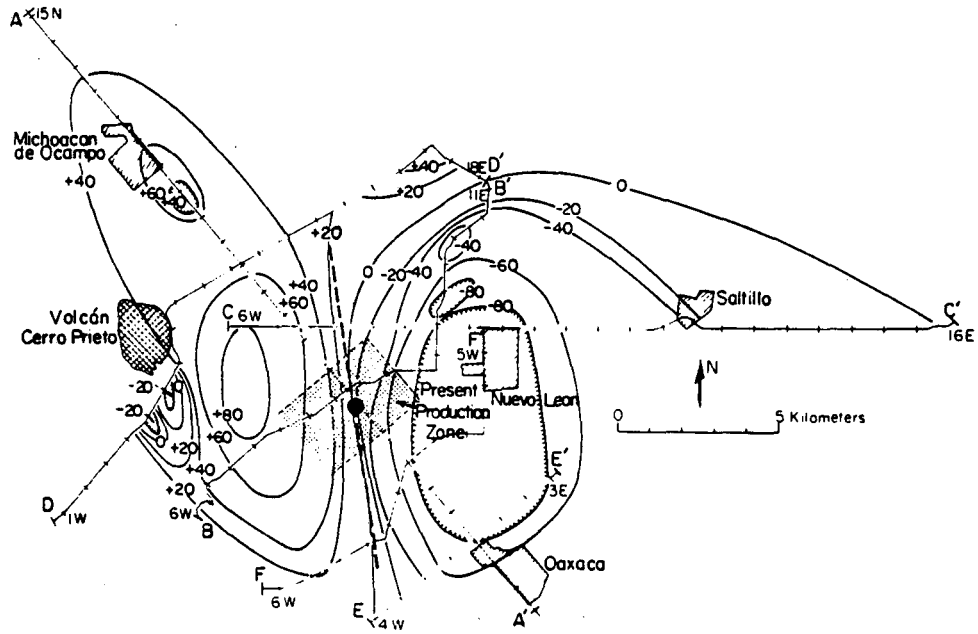
XBL 787-5328 A

Figure 1.   The 1978 Cerro Prieto SP contour map (contour interval = 20 mV)

Figura 1.   Cerro Prieto. Contornos de potencial natural para 1978 (Intervalo entre contornos: 20 mV).
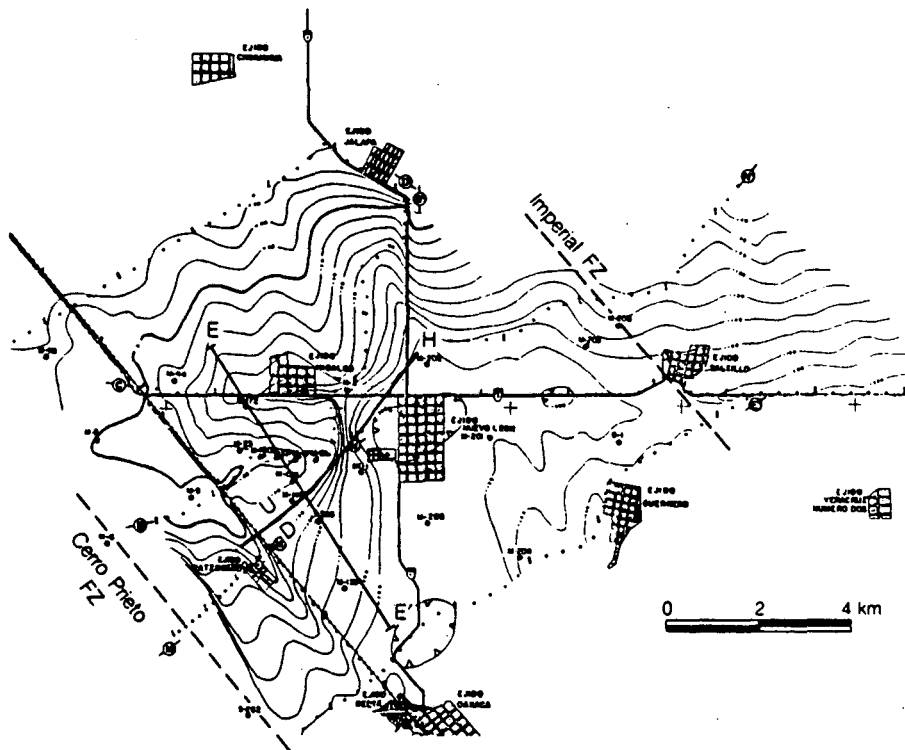
XBL 891-218A

Figure 2.   The 1988 Cerro Prieto SP contour map showing the trace of Fault H at the depth of the β reservoir (contour interval = 10 mV).

Figura 2.   Cerro Prieto. Contornos de potencial natural para 1988 (Intervalo entre contornos: 10 mV). Se indica también la traza de la Falla H al nivel del yacimiento β.
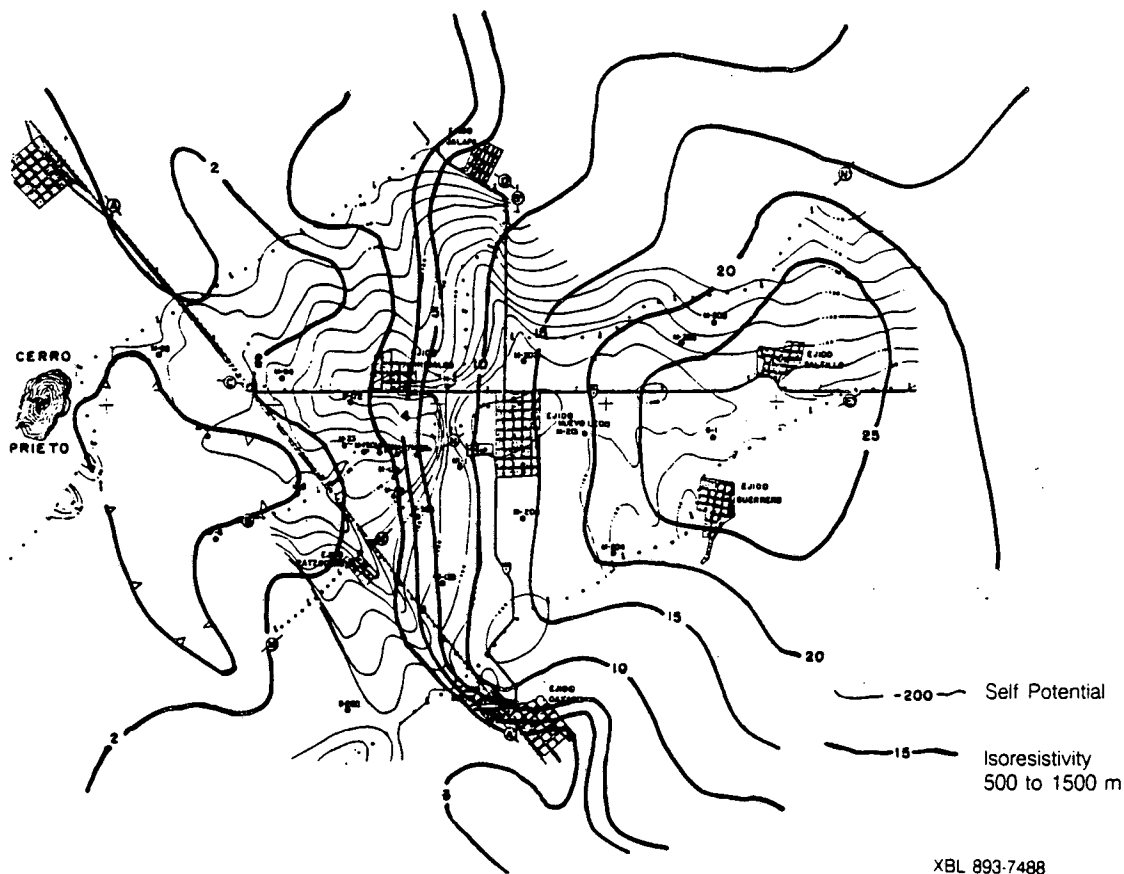
Figure 3. The 1988 Cerro Prieto SP contour map plotted with the isoresistivity contours based on Schlumberger soundings. The resistivities are average values for the 500- to 1500-m depth range.

Figura 3. Cerro Prieto. Contornos de potencial natural para 1988 y contornos de isoresistividad basados en sondeos Schlumberger. Las resistividades son valores promedios para el intervalo entre 500 y 1500 m de profundidad.

Because migration along a chemical gradient proceeds differently for different ions, a charge separation occurs together with the creation of a small voltage counter-force. Assuming NaCl is the only salt in solution, the voltage V_l across an ideal liquid junction can be expressed as

$$V_l = -\frac{RT}{F} (2 t_{Na} - 1) \ln (\frac{a''}{a'}), \qquad (1)$$

where R is the gas constant (8.3144 J/mol · K), F is Faraday's constant (96,487 coulomb/mol), T is temperature (K), t_{Na} is the transport number of Na^+ (approximately 0.4), and a′, a″ are the activities in the dilute (a′) and concentrated (a″) solutions (Hearst and Nelson, 1985). Next, if we assume that the activity ratio is equal to the concentration ratio, we can express V_l in terms of a pore water resistivity ratio as

$$V_l = - \frac{RT}{F} (2t_{Na} -1) \ln (\frac{\rho'}{\rho''}), \qquad (2)$$

where $\rho'/\rho'' \approx 10$ can be inferred from the bulk rock resistivity values shown in Figure 3. Plugging the appropriate numbers into Equation 2 we find that the sign change of the

voltage matches the SP field data, but the magnitude of the liquid junction SP voltage is only about 13 mV for water at 50°C (323K), and 15 mV at 100°C. Thus, a liquid junction diffusional potential due to the shallow mixing of groundwater derived mainly from the Colorado River and thermal waters probably accounts for less than about 10 percent of the measured SP variation.

Electrokinetic Effects

To determine whether the 1988 SP data are, in fact, production related, we attempted to numerically model the SP using known production data for the month of the survey, the hydrogeologic-lithofacies model for the system, and the subsurface geophysical parameters, either measured directly (electrical resistivity and temperature) or inferred from reservoir models (permeability). Thus far, we have focussed our attention on a single northwest-southeast trending profile, Line E–E′, for which there is a lithofacies cross-section and a recently updated model of geothermal fluid flow (Halfman et al., 1986b). In addition, the profile is roughly normal to the steepest SP gradients, and it crosses an area of significant geothermal production. Figure 4 shows the simplified lithofacies section, with the interpreted geothermal fluid flow
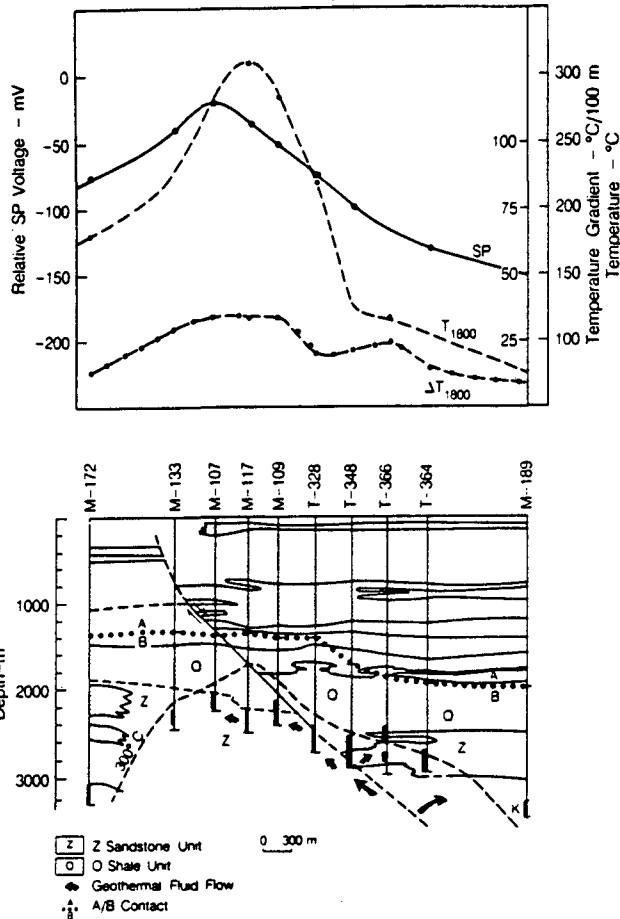
Figure 4. Simplified lithofacies section for the north-south Line E–E' (after Halfman et al., 1986b). Also shown is the SP voltage profile plotted against the subsurface temperature and temperature gradient at 1800 m depth.

Figura 4. Sección simplificada de litofacies en dirección norte-sur a lo largo de la linea E-E'(de Halfman et al., 1986b). También se muestra el perfil del voltaje de potencial natural versus la temperatura en el subsuelo y el gradiente térmico a 1800 m de profundidad.

patterns, and the geothermal production intervals. Northwest of Fault H production is from the upthrown side of the β reservoir in Sand unit Z, at a depth of approximately 2.2 km. Southeast of Fault H production comes mainly from a depth of 2.6 to 2.8 km in the downthrown Sand Z unit. Temperatures in the β reservoir are 320-350°C. Less is known about the deeper γ reservoir (unit K) and so it has been excluded from this study.

To calculate the surface SP along hydrogeologic profile E–E' we used a modified version of the program SPXCPL written by Sill and Killpack (1982). A complete discussion of the basis for these calculations is beyond the scope of this paper (see for example Nourbehecht, 1963; Sill, 1983b), so it shall suffice to say that SPXCPL solves separately for the electric potentials in the earth subject to a distribution of pressure (flow or electrokinetic) sources and thermal (ther-

moelectric) sources. SPXCPL solves the 2-D coupled flow problem by explicitly modeling the primary flows (fluid flux and heat flux) and the induced secondary electric potentials that arise from those flows (Onsager, 1931).

Figure 5 shows the flow model constructed and used, and Table 1A lists the final set of parameters for the model. The electrical resistivity values are reasonably well constrained by surface and borehole surveys and so these values were kept fixed for the calculations. The lithologic unit permeabilities are an important adjustable parameter in the calculations. After several trials we found that a permeability value of approximately the average of the horizontal and vertical permeabilities used by Halfman et al. (1986a) and Halfman et al. (this volume) for their reservoir modeling studies gave electric potentials close to those observed. The final set of permeabilities values used in the calculations are listed in Table 1A. Also listed are the electrokinetic coupling coefficients used. This parameter was also allowed to vary, but only within the ranges for sands and shales.

To complete the model, we introduced several fluid point sources and sinks. Two large sinks (negative pressure sources) account for well production from the upthrown and downthrown sides of the β reservoir during March 1988. Source II represents the total fluid flow rate of 780 L/s produced from a group of wells near E–E'. Source IV represents the effect of fluid produced from another group of wells on the downthrown side of the β reservoir, and yielding a total of 1000 L/s. To simplify the model we lumped well production into only the two sinks, and we assume that little or no boiling occurs in the reservoir even though there is evidence for boiling in the upthrown side of the β reservoir (de León Vivar, 1988). In addition to the fluid sinks, we initially specified four positive pressure sources to simulate recharge effects. Sources I (100 L/s) and VI (1000 L/s) represent lateral recharge to the β reservoir, and V (100 L/s) represents a source of deep, hot water recharge guided by the H fault, as indicated by the flow arrows in Figure 4. These three recharge sources total 70% of the fluids produced by the wells closest to E–E'. Additionally, we introduced a source of shallow cold water recharge, Source VII (100 L/s), to be consistent with the electrical resistivity model (Wilt and Goldstein, 1981) and the hydrothermal flow model (Elders et al., 1984) which indicates shallow recharge of Colorado River groundwater from the east into the α reservoir.

Holding source-sink magnitudes constant and varying only permeability and coupling coefficients, we obtained a reasonable fit (Curve 60 in Fig. 6) to the observed SP profile after only a few iterations. Additional calculations were then run to test the sensitivity of the SP voltage profile to the locations and magnitudes of recharge pressure sources.

The SP low in the southeast part of the survey area requires both shallow lateral fluid flow in Unit 2 and deeper lateral recharge in the Z Sand unit from the southeast. The match between observed and calculated voltages improved after we eliminated recharge Source I, simulating lateral recharge in the Z Sand from the northwest (Curve 61). The match improved more after we eliminated source V which simulates deep vertical recharge to the β reservoir (Curve 62). Thus, on the basis of electrokinetic potentials alone, it
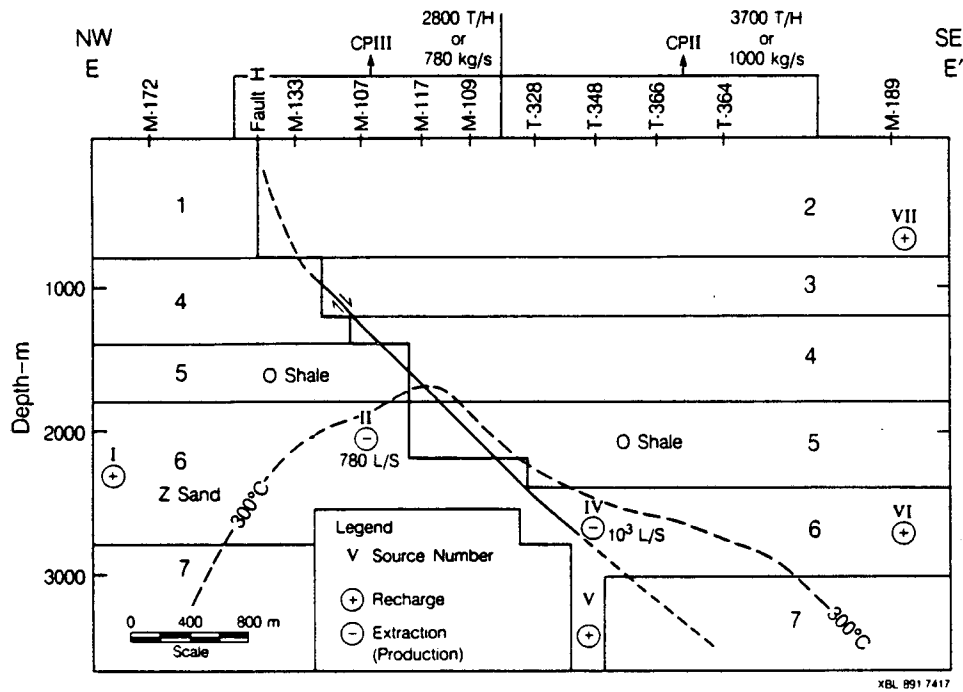
Figure 5. Two-dimensional mass flow model used to model electrokinetic effects
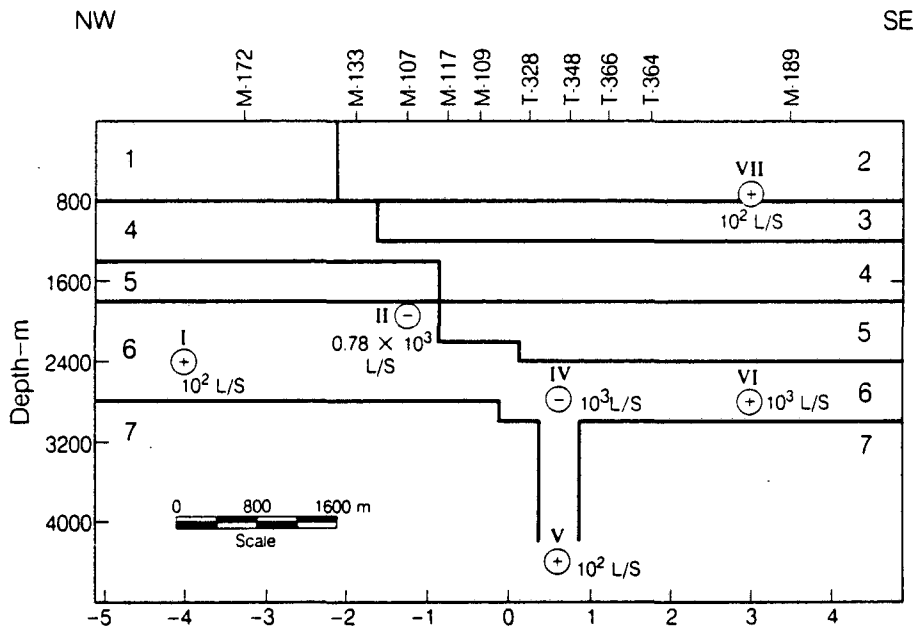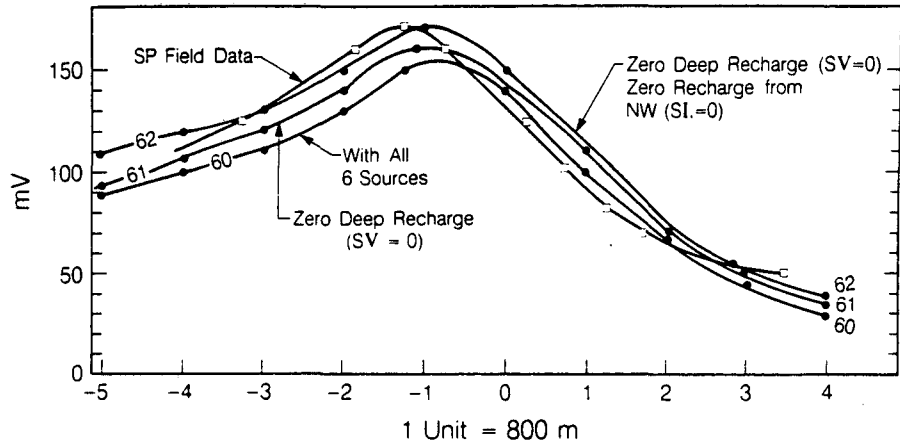arising from point sinks of fluid withdrawal and point sources of fluid
recharge.

Figura 5. Modelo bidimensional de flujo másico utilizado en el modelado de efectos
electrocinéticos asociados con puntos de recarga y descarga de fluidos.

Table 1A. Unit Parameters for Cerro Prieto SP Model: Pressure Sources

Unit	Geologic Designation	Electrical Resistivity (ohm-m)	Permeability (md)	Electrokinetic Coupling Coeff. (mV/atm)
1		2	10	5
2		20	50	20
3		6	10	5
4		0.5	50	50
5	Shale O	6	0.5	5
6	Sand Z	3	50	100
7		10	5	5

Table 1B. Unit Parameters for Cerro Prieto SP Model: Thermal Sources

Unit	Geologic Designation	Electrical Resistivity (ohm·m)	Thermal Conductivity (W/m·°C)	Thermoelectric Coupling Coeff. (mV/°C)
1		2	2	0.05
2		20	2	0.10
3		6	2	0.30
4		0.5	2	0.10
5	Shale O	6	1.8	0.30
6	Sand Z	3	2	0.10
7		10	2.5	1.00

Figure 6. Numerical model results for different cases of recharge. Horizontal distance resolution is 200 m.

Figura 6. Resultados del modelado numérico para diferentes casos de recarga. La resolución para distancias horizontales es de 200 m.

Thermoelectric Potentials

To see how much the SP data may have been influenced by thermoelectric currents, we next calculated the voltages due to a distribution of thermal sources using program SPXCPL. A reasonable fit to the subsurface temperature distribution was obtained by distributing 70 sources, each 0.25 x 10^6 watts, within the region outlined in Figure 7. The rock thermal parameters shown in Table 1B were used in the model. Although a closer fit to subsurface temperatures could have been achieved by expanding the thermal zone to the northwest, the numerical exercise was concluded when it became apparent that the peak thermoelectric voltage at the surface would not exceed 4 mV, which is within the noise level of the field data.

Discussion of the SP Model

Our numerical calculations indicate that most of the observed 1988 SP anomaly can be accounted for by a set of fluid flow point sources that approximate actual well production and simulate recharge effects. The best fit to the SP profile (Curve 62 in Fig. 6) was obtained for a flow model with zero (or negligible) lateral recharge to the upthrown side of the β reservoir from the north-northwest, and negligible hot water recharge from a presumed deep aquifer. The SP anomaly, however, requires lateral recharge from the
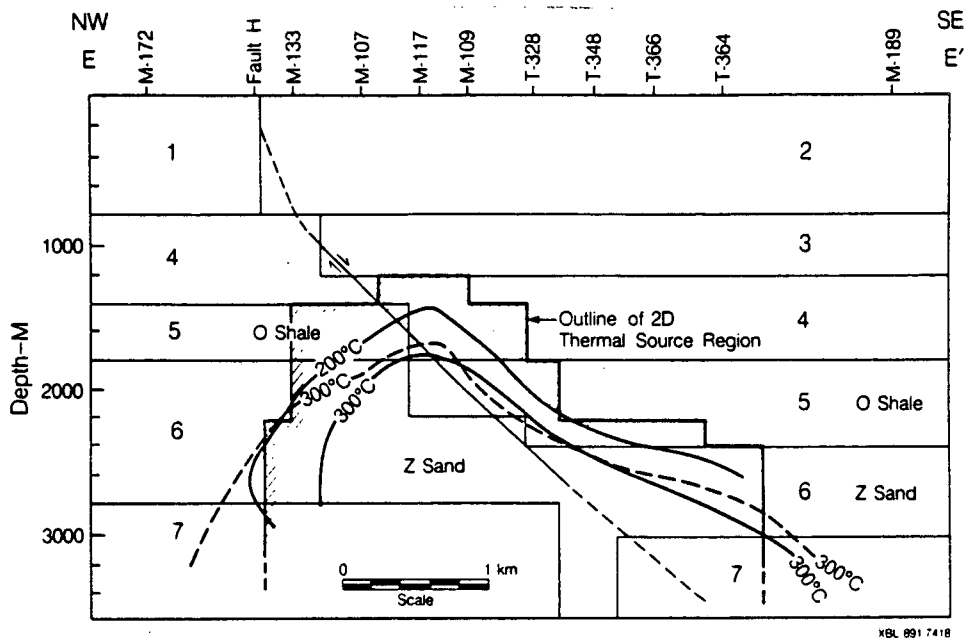
It would appear that the observed SP anomaly may be explained by a reservoir exploitation model in which most of the β reservoir recharge flows from the southeast.

XBL 891 7418

Figure 7. Two-dimensional thermal model for Cerro Prieto used to calculate ther-moelectric SP voltages. Seventy point sources, 0.25 x 10⁶W each were used, but produce only a broad negative anomaly of < 4 mV (peak). The solid isotherm lines are calculated, the dashed line is the observed 300°C isotherm.

Figura 7. Cerro Prieto. Modelo bidimensional térmico utilizado para calcular voltajes de potencial natural termoeléctricos. Se usaron setenta fuentes puntuales de 0.25 x 10⁶ W cada una, obteniéndose sólo una amplia anomaliá nega-tiva menor de 4 mV (cresta). Las líneas contínuas indican isotermas calcu-ladas, la línea punteada corresponde a la isoterma observada de 300°C.

southeast. Most of this flow occurs in the Z sand and seems to be approximately equal to the fluid extraction rate from the wells producing from the down-dropped side of the β reser-voir. This cold water recharge from the southeast also helps to explain the subsurface temperature pattern (Fig. 7). We also include a source of shallow water recharge to account for an eastward flow of groundwater that recharges the shal-low α reservoir (not shown in section E–E').

It is clear from Curve 62 in Figure 6 that we have a fair, but by no means exact, match to the observed data. A marginally better match might be obtained by introducing a liquid junction potential represented by a shallow vertical source plane passing beneath well M-117. As discussed ear-lier, a vertical liquid junction should theoretically cause a dipolar anomaly of the right polarity which, with proper placement, would shift Curve 62 into better agreement with the observed curve. In addition, the mismatch on the SE limb of the anomaly could be further decreased by means of fine tuning the locations and magnitudes of the recharge sources.

Although these manipulations are contrived, we nevertheless believe that our simple electrokinetic model gives a reasonable explanation for production-related fluid flows. Independent reservoir modeling by Ocampo et al. (this volume) and Halfman-Dooley et al. (this volume) and fluid geochemistry-enthalpy studies by Truesdell et al. (this volume) also seem to show that the upthrown side of the β reservoir is not receiving adequate natural fluid recharge.

Conclusions

A repeat SP survey over the Cerro Prieto geothermal field shows a number of differences from the survey made 10 years earlier. Part of the differences can be attributable to better data quality and higher data density of the recent sur-vey. Numerical calculations indicate that a minor part of the SP anomaly may be caused by thermoelectric and liquid junction potentials. Most of the anomaly amplitude and the shift in anomaly position can be explained by production-recharge effects. At the time of the initial survey in 1978 production for the CPI plant came from the shallow α reser-voir with thermal fluid recharge ascending a "sandy gap" in the otherwise impermeable Shale O unit. At the time of the resurvey in March 1988, production had been greatly expanded to the east. Most of the fluids produced are now from the deeper β reservoir. A numerical model for electrok-inetic SP currents fits the 1988 production data and the current hydrogeologic model reasonably well. One of the important findings from the modeling exercise is the sensi-tivity of the SP to recharge. Calculations show that in response to production the β reservoir is being recharged mainly by lateral flow within the Z sand coming from the east-southeast. Restated, the SP modeling indicates that fluid recharge to the down-thrown side of the β reservoir is approximately equal to fluid production from that part of the reservoir. On the other hand, the SP electrokinetic model suggests there is negligible natural recharge to the Z sand, β

reservoir on the upthrown side of the H fault. These findings seem to be consistent with independent reservoir analyses reported at this Symposium by other workers.

Acknowledgments

References

Arellano G., J. F., and Rodríguez B., J., 1989, "Características generales del segundo levantamiento de potencial natural en el Campo Geotémico de Cerro Prieto," this volume.

Corwin, R. F. and Hoover, D. B., 1979, "The Self Potential Method in Geothermal Exploration," *Geophysics*, **44**, 226-245.

Corwin, R. F., Morrison, H. F., Díaz, C. S. and Rodríguez B., J., 1978, "Self-Potential Studies at the Cerro Prieto Geothermal Field," Proc. First Symp. on the Cerro Prieto Geothermal Field, Baja California, Mexico, Lawrence Berkeley Laboratory, LBL-7098, 204-210.

de León Vivar, J., 1988, "Presencia de dos fases en el yacimiento del campo geotermico de Cerro Prieto", *Geotermia, Rev. Mex. de Geoenergíd*, **4**, 203-211.

Elders, W. A., Bird, D. K., Williams, A. E. and Schiffmann, P., 1984, "Hydrothermal flow regime and magmatic heat source of the Cerro Prieto geothermal system, Baja California, Mexico," *Geothermics*, **13**, 27-47.

Halfman, S. E., Lippmann, M. J. and Bodvarsson, G. S., 1986a, "Quantitative Model of the Cerro Prieto Field," Proc. 11th Workshop Geothermal Reservoir Engin., Stanford Univ., SGP-TR-84, 127-134.

Halfman, S. E., Mañon, A. and Lippmann, M. J., 1986b, "Update of the Hydrogeologic Model of the Cerro Prieto Field Based on Recent Well Data," Trans. Geothermal Resources Council, **10**, 369-376.

Halfman-Dooley, S. E., Lippmann, M.J. and Bodvarsson, G. S., 1989, "Progress report on LBL's numerical modeling studies on Cerro Prieto," this volume.

Hearst, J. R. and Nelson, P. H., 1985, "Well logging for physical properties," McGraw-Hill, New York, 571 p.

Ishido, T., Mizutani, H. and Baba, K., 1983, "Streaming Potential Observations, using Geothermal Wells and In-Situ Electrokinetic Coupling Coefficients under High Temperatures," *Tectonophysics*, **91**, 89-104.

Ishido, T., Kikuchi, T. and Sugihara, M., 1987, "The Electrokinetic Mechanism of Hydrothermal-Circulation-Related and Production-Induced Self Potentials," Proc. 12th Workshop Geothermal Reservoir Engin., Stanford Univ., SGP-TR-109, 285-290.

Lippmann, M. J., Truesdell, A. H., Mañon, A., and Halfman, S. E., 1989, The hydrogeologic geochemical model of Cerro Prieto Revisited: Lawrence Berkeley Laboratory, LBL-26819, presented at the 14th Workshop Geoth. Reserv. Engin., Stanford Univ., Jan. 24-26.

Nourbehecht, B., 1963, "Irreversible Thermodynamic Effects in Inhomogeneous Media and their Applications to Certain Geoelectric Problems," Unpub. Ph.D. thesis, MIT, Cambridge, MA.

Ocampo, J. D. D., Ayuso, M. A., Pelayo, L., A., 1989, "Modelado del campo geotérmico de Cerro Prieto," this volume.

Onsager, L., 1931, "Reciprocal Relations in Irreversible Processes I," *Phys. Rev.*, **37**, 405-426.

Sill, W. R., 1983a, "Final Report, Interpretation of Self-Potential Measurements during Injection Tests at Raft River, Idaho," Earth Sciences Laboratory, Univ. Utah Res. Inst., DOE/ID/12709-103, ESL-120, 20 p.

Sill, W. R., 1983b, "Self-Potential Modeling from Primary Flows," *Geophysics*, **47**, 76-86.

Sill, W. R. and Killpack, T. J., 1982, "SPXCPL: Two-Dimensional Modeling Program of Self-Potential Effects from Cross-Coupled Fluid and Heat Flow," Univ. of Utah Res. Inst., DOE/ID/12079-60, ESL-74, 26 p.

Truesdell, A. H., Terrazas, B., Hernández, L., Janik, C., Quijano, L. and Tovar, R., 1989, "The response of the Cerro Prieto reservoir to exploitation as indicated by fluid geochemistry", this volume.

Wilt, M. J. and Goldstein, N. E., 1981, "Resistivity monitoring at Cerro Prieto," *Geothermics*, **10**, 3/4, 183-194.